Article

Current Biology

# The Venus Flytrap *Dionaea muscipula* Counts Prey-Induced Action Potentials to Induce Sodium Uptake

## Highlights

- Carnivorous *Dionaea muscipula* captures and processes nutrient- and sodium-rich prey
- Via mechano-sensor stimulation, an animal meal is recognized, captured, and processed
- Mechano-electrical waves induce JA signaling pathways that trigger prey digestion
- Number of stimulations controls the production of digesting enzymes and uptake modules

## Authors

Jennifer Böhm, Sönke Scherzer, Elzbieta Krol, ..., Sergey Shabala, Erwin Neher, Rainer Hedrich

## Correspondence

eneher@gwdg.de (E.N.), hedrich@botanik.uni-wuerzburg.de (R.H.)

## In Brief

Children are able to count at the age of 15–18 months. In this work, Böhm et al. demonstrate that the carnivorous Venus flytrap plant is able to count as well. The leaf tips develop into snap traps, where the number of contacts of the prey with mechano-sensitive trap initiates capturing and processing of the animal victim.

Böhm et al., 2016, Current Biology *26*, 286–295
February 8, 2016 
http://dx.doi.org/10.1016/j.cub.2015.11.057

CellPress

CellPress

Current Biology
Article

# The Venus Flytrap *Dionaea muscipula* Counts Prey-Induced Action Potentials to Induce Sodium Uptake

Jennifer Böhm,[1,8] Sönke Scherzer,[1,8] Elzbieta Krol,[1] Ines Kreuzer,[1] Katharina von Meyer,[1] Christian Lorey,[1,2] Thomas D. Mueller,[1] Lana Shabala,[3] Isabel Monte,[4] Roberto Solano,[4] Khaled A.S. Al-Rasheid,[1,5] Heinz Rennenberg,[6] Sergey Shabala,[3] Erwin Neher,[7,*] and Rainer Hedrich[1,*]

[1]Institute for Molecular Plant Physiology and Biophysics, Julius-von-Sachs Platz 2, 97082 Würzburg, Germany
[2]Naturwissenschaftliches Labor für Schüler, Friedrich-Koenig-Gymnasium, 97082 Würzburg, Germany
[3]School of Land and Food, University of Tasmania, Hobart, TAS 7001, Australia
[4]Plant Molecular Genetics Department, National Centre for Biotechnology (CNB), Consejo Superior de Investigaciones Científicas (CSIC), Campus University Autónoma, 28049 Madrid, Spain
[5]Zoology Department, College of Science, King Saud University, P.O. Box 2455, Riyadh 11451, Saudi Arabia
[6]Institute of Forest Sciences, University of Freiburg, Georges-Koehler-Allee 53/54, 79085 Freiburg, Germany
[7]Department for Membrane Biophysics, Max Planck Institute for Biophysical Chemistry, 37077 Goettingen, Germany
[8]Co-first author
*Correspondence: eneher@gwdg.de (E.N.), hedrich@botanik.uni-wuerzburg.de (R.H.)
http://dx.doi.org/10.1016/j.cub.2015.11.057


## SUMMARY

**Carnivorous plants, such as the Venus flytrap (*Dionaea muscipula*), depend on an animal diet when grown in nutrient-poor soils. When an insect visits the trap and tilts the mechanosensors on the inner surface, action potentials (APs) are fired. After a moving object elicits two APs, the trap snaps shut, encaging the victim. Panicking preys repeatedly touch the trigger hairs over the subsequent hours, leading to a hermetically closed trap, which via the gland-based endocrine system is flooded by a prey-decomposing acidic enzyme cocktail. Here, we asked the question as to how many times trigger hairs have to be stimulated (e.g., now many APs are required) for the flytrap to recognize an encaged object as potential food, thus making it worthwhile activating the glands. By applying a series of trigger-hair stimulations, we found that the touch hormone jasmonic acid (JA) signaling pathway is activated after the second stimulus, while more than three APs are required to trigger an expression of genes encoding prey-degrading hydrolases, and that this expression is proportional to the number of mechanical stimulations. A decomposing animal contains a sodium load, and we have found that these sodium ions enter the capture organ via glands. We identified a flytrap sodium channel DmHKT1 as responsible for this sodium acquisition, with the number of transcripts expressed being dependent on the number of mechano-electric stimulations. Hence, the number of APs a victim triggers while trying to break out of the trap identifies the moving prey as a struggling $Na^+$-rich animal and nutrition for the plant.**

## INTRODUCTION

During evolution, plants developed senses to recognize mechanical forces. Such forces can be imposed on plants from environmental clues such as wind and barriers in the soil to animal movement and herbivory. The touch causes an immediate rise in jasmonic acid (JA) biosynthesis [1–3].

The model plant species *Arabidopsis* senses touch without any specialist cell types or organs. Tendrils of climbing plants, however, have specialized buds that allow a conversion of already weak mechanical forces into a curvature of the climbing organ toward a given support. A similar tendril response can be elicited when, in the absence of touch, jasmonates are administered [4]. Like climbing plants, some carnivorous plants are also equipped with the sophisticated mechano-sensory structures and touch signaling mechanisms [5–7].

When Charles Darwin observed the Venus flytrap, *Dionaea muscipula*, he was fascinated by this plant's ability to sense and catch animals to circumvent the limitations of its nutrient-poor habitat [8]. The tips of *Dionaea* leaves have developed into bilobed snap trap-type capture organs, equipped with a number of mechano-sensitive hairs and a densely packed array of glands. Insects are attracted to the capture organs by a fruity volatile blend emitted by starving flytraps [9]. Visitors searching for food eventually touch the trigger hairs leading to the electric excitation of the trap; the mechanical stimulus is converted into an all-or-nothing action potential (AP). Once two APs are elicited within 15–20 s of each other, the trap lobes close within a fraction of a second [5]. Ongoing mechanical stimulation of the trigger hairs by the insect as it tries to escape initiates the hermetical sealing of the capture organ into a green stomach. Secretion of acid and digestive enzymes into the stomach breaks the entire

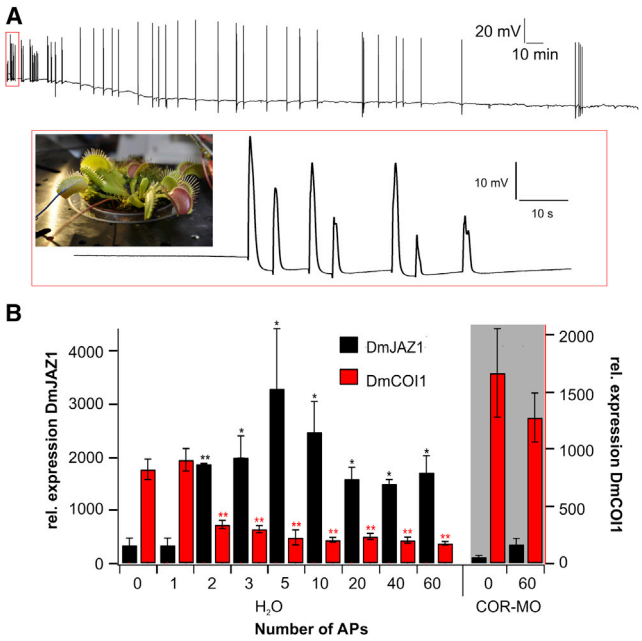


**Figure 1. Prey-Evoked APs Regulate Gene Expression**

(A) Surface potential recordings from the surface of a Venus flytrap lobe during cricket capture. During the first hour, 51 APs were elicited, and within 6 hr of measurement, more than 100 APs were recorded. The inset (red frame, enlarged in the lower panel) shows the first seven APs that lead to prey capture and initiation of digestion. The picture shows a *Dionaea* plant with attached surface electrode to a trap lobe. The presented graph is representative of five individual experiments.

(B) Quantification of DmJAZ1 (left axis, black bars) and DmCOI1 (right axis, red bars) transcript levels in response to the number of elicited APs (as indicated). Traps were pre-treated 4 hr before application of APs with $H_2O$ (shaded in white) or 100 μM COR-MO (shaded in gray). Transcript numbers are given relative to 10,000 molecules of DmACT1. Asterisks indicate a statistically significant difference to zero applied APs (*$p < 0.05$; **$p < 0.01$ by one-way ANOVA) ($n \geq 6$, mean ± SE).

See also Figure S1.

insect down. By establishing this outstanding apparatus, carnivorous plants are able to ingest the prey's components. In addition to carbon, nitrogen, phosphate, and sulfur, substantial amounts of potassium and sodium are also contained in the prey [10–12]. In this study, we consider whether the Venus flytrap uses the number of prey-triggered APs to identify visitors as food sources, to capture and to process them, and to internalize nutrient cations from the prey. We found that by counting and integrating the mechano-electric signals elicited by the trapped prey, *Dionaea muscipula* triggers biosynthesis of the touch hormone jasmonate, secretion of lytic enzymes, and channel-mediated uptake of prey nutrient-associated sodium loads.

## RESULTS

### Insect Capture Electrically Excites the Venus Flytrap

In order to investigate the Venus flytrap's signaling cascade involved in the prey capturing and digestion, we monitored the electrical activity of a prey-catching flytrap via surface electrode measurements. For these experiments we used crickets (*Acheta domesticus*) 6–12 mm in length and with an average weight of 23.8 mg. It is well known that only two stimuli are sufficient for provoking fast trap closure, thereby capturing the insect [5]. Once trapped, the still-moving victim continues to activate these mechanosensors, prolonging the electrical stimulation for many hours (Figure 1A). In these experiments, we recorded 63 ± 13 APs during the first hour after prey capture (n = 5, mean ± SE).

### Mechano-electric Signals Are Translated into JA Biosynthesis and Hydrolase Production

In a previous study, we showed that when a second AP quickly follows the first, the rapid trap closure is provoked, but there is no increase in the cytoplasmic calcium level in the gland cells. The subsequent AP arrival at the gland, however, elicits a calcium spike [5]. There is evidence from non-carnivorous plants that increases in cytosolic calcium triggers JA biosynthesis [13–16], and, for Venus flytrap, studies have already shown that insect stimulation is associated with a 2-fold increase in jasmonates within just 30 min of prey capture [5, 6, 17]. To explore this association more fully, we sought to simulate the movements of prey in the capture organ and to record the resulting electrical response. As shown in the picture in Figure 1A, we attached a surface electrode to the trap lobes and mechanically stimulated the trigger hairs for up to 60 times per hour. To mimic the action of an insect, we simulated the situation with a captured insect by manual application of APs. Note that after the first applied AP, the trap was still open; to close the trap, the first and second stimuli needed to be consecutively applied, and both needed to elicit an AP. In the closed "prey capture" state, as with the insect in Figure 1A, we applied additional stimuli, one per minute, which could be registered as the fired signal between AP numbers 3 to 60 (cf. for 2 and 5 stimuli in Figure 1B).

Four hours after the first applied AP, we collected trap samples and monitored the expression of JA genes alongside those of the stomach hydrolases and solute transporters. To quantify the dose dependency, we used qPCR to track the association between the number of APs and the expression of the genes selected.

To analyze JA signaling in active traps, we focused on the first elements in the pathway JA receptor COI1 (CORONATINE INSENSITIVE 1) and its co-receptor JAZ1 (JASMONATE ZIM DOMAIN 1) [1, 18, 19]. JA-Ile binds to the COI1 receptor, which facilitates the formation of COI1-JAZ complexes. This leads to ubiquitination and subsequent degradation of the co-receptor JAZ1 [20–22]. We first measured the resting level of DmJAZ1 (GenBank: KT223139) in untreated (no mechanical stimulation) traps and found 341 ± 131 transcripts/10,000 DmACT, after which we stimulated the plants. This stimulation resulted in an increase in gene expression in the manner proportional to the number of trigger-associated APs. The first two applied APs, which close the trap, increased the DmJAZ1 transcript levels as much as 5.5-fold compared to unstimulated traps. With more than five APs elicited, JA gene-associated transcripts tended toward maximal levels (Figure 1B, black bars). In contrast to JAZ1, we found DmCOI1 (GenBank: KT223140) already expressed in resting traps, but after two AP stimulations, its transcription was significantly repressed (Figure 1B, red bars). As in non-carnivorous *Arabidopsis* plants [18, 23–26], JAZ1 induction indicates that the JA-signaling pathway is mechanically induced.

Also, in the *Arabidopsis* system, mechanical wounding associated with herbivore foraging has been shown to induce the expression of defense genes, including a set of hydrolases [18, 27–29]. The Venus flytrap shows behavior comparable to the wounding response of *Arabidopsis* when the captured prey is recognized as a profitable nutrient source. A previous study has shown that mechanical stimulation of the Venus flytrap, by either an insect or the experimenter, induces gland cells to secrete a cocktail of lytic enzymes [30]. Accordingly, we have selected three hydrolases for further transcript profiling: the SAG12 (GenBank: KT223141) and SCPL49 (GenBank: KT223142) protease as well as the VF chitinase-I [31]. These proteins are highly abundant in the green stomach formed by the closed trap lobes [30]. Our present results indicate that transcription of the *Dionaea* hydrolases is also dependent on the number of mechano-electric signals, but with five APs necessary for significant gene expression, the tested hydrolases seem to follow the JA-signaling expression (Figure S1A). It appears that *Dionaea* may control the amount of lytic enzymes produced in and secreted by the gland cells via the number of electrical signals activating the JA pathway. To test this assumption, we treated the flytrap with JA-Ile, the physiologically active form of JA, and its molecular mimic COR (coronatine), in the absence of any mechano-electric stimulation. Metabolic conversion of JA-Ile to hydroxylated 12-hydroxy-JA-Ile appears to inactivate JA signaling [32–34]. Therefore, as a control, we applied $H_2O$, 12-hydroxy-JA-Ile, and ethynyl-In-Ile, two isoleucine derivatives that are inactive in floral and extra-floral nectary glands [35, 36] as well as in flower and seed development [37]. When sprayed on open traps, JA-Ile and COR, but not $H_2O$, 12-hydroxy-JA-Ile, or ethynyl-In-Ile, induced slow trap closure, secretion (cf. [5]), and transcription of hydrolases (Figure S1B). These effects were consistent with the trigger-hair-based electrostimulation of the green stomach (Figure S1A).

We have shown that in the flytrap, similar to other plant systems, COR is the only compound with JA-Ile agonistic activity. Recently it was shown that the COR derivative coronatine-O-methyloxime (COR-MO) reverts the effects of JA-Ile and COR treatments [38]. To dissect the JA pathway in the *Dionaea* system, we synthesized COR-MO and pre-treated flytraps with the JA inhibitor prior to trigger-hair stimulation. Figure 1B (shaded in gray) shows that COR-MO prevents the response of DmCOI1/DmJAZ1 and stomach hydrolases (Figure S1A) to mechano-electric stimulation. Even after the application of as many as 60 APs, no significant gene regulation was detectable when the JA inhibitor was applied (gray bars). This indicates that a touch to the trigger hair is converted into an electrical signal, which, when received at the level of the gland cells, induces prey decomposition via the JA pathway. But what are the pathways for the uptake of prey-derived solutes?

## Stimulated Flytraps Take Up Prey-Derived Sodium

Humans gain the sodium ions required for electrical excitability (i.e., APs) to a large extent from a meat diet [39, 40]. In the context of flesh-eating plants, we postulated whether *Dionaea* takes advantage of prey-available $Na^+$. If this is the case, the question is does it affect the AP? To monitor how a flytrap handles a sodium-rich meal, we monitored the movement of the positive-charged sodium ion and $Na^+$-induced membrane responses of gland cells in *Dionaea's* "green stomach." For sodium uptake experiments, we used a standardized animal powder with a defined ion content (Table S1) [41]. This fodder paste with a $Na^+$ concentration of ~5 mM was applied to the inner trap surface, whereupon the sensory hairs were stimulated to close the trap and initiate digestion. By sampling the green stomach, we determined the time-dependent changes in trap sodium content by inductively coupled plasma optical emission spectroscopy (ICP-OES). We found that the level of sodium started to rise >6 hr after initiating feeding. It reached an increased steady state at 12–24 hr, lasting for at least 2–3 days (Figure 2A). This steady-state $Na^+$ content of the fed trap was about twice that of control traps (at t = 0 hr) and those only fed for 6 hr. In contrast to the sodium accumulation in the trap, feeding did not increase the sodium content of the petiole significantly (Figure 2A, red bars). This indicates that *Dionaea* takes up and retains sodium in the capture organ. To confirm this finding and to study the sodium intake at a higher resolution, we focused on the ~37,000 glands covering the trap's inner surface. Each gland is engaged with the secretion of digestive fluid and uptake of nutrients [42]. Given that COR triggers processes similar to those activated by a natural prey, we used sodium-free, chemically well-defined JA mimic to study the sodium transport into glands. We stimulated gland cells with COR in the presence of 1.15 μmol sodium, the approximate load carried by a fly [11, 43]. As a result, the sodium content in *Dionaea* gland cells increased 7-fold after 3 days of digestion (Figure 2B).

## Sodium Ions Depolarize Activated Gland Cells

To follow the $Na^+$ response of the gland cell's membrane, we used intracellular voltage-recording electrodes. Single trap lobes were fitted into a perfusion chamber, and the electrical response to $Na^+$ loads was recorded (cf. [44, 45]). In the initial set of experiments, glands of traps that had not been previously stimulated by a prey were challenged with buffers containing up to 120 mM $Na^+$ (approximately the sodium concentration of our blood). During the stepwise increase in extracellular $Na^+$, the glands were depolarized from −116 ± 19 mV to −99 ± 6 mV and finally to −82 ± 9 mV (Figure 2C). In a complementary set of experiments, sodium was applied to traps previously stimulated by living insects (cf. [30]). When compared to non-triggered glands, those previously stimulated exhibited more pronounced $Na^+$-dependent depolarizations. Such "activated" gland cells depolarized in response to 120 mM $Na^+$ from −122 ± 14 mV to −41 ± 29 mV.

To elucidate the affinity of the $Na^+$ transporter more precisely, we applied a $Na^+$ protocol of nine steps with $Na^+$ concentrations ranging from 0.3 to 120 mM, both in prey-stimulated and non-stimulated gland cells. Plotting the steady-state depolarization as a function of the substrate concentration resulted in a $Na^+$ saturation curve that could be best fitted using a Michaelis-Menten function. In non-stimulated traps, a $_{\Delta}V_{max}$ at 120 mM $Na^+$ of 37 mV and an apparent half maximal effective concentration ($EC_{50}$) of about 21 mM was derived, while in gland cells from "stomach"-forming, digesting traps, the maximum membrane depolarization at 120 mM $Na^+$ was about 80 mV, and the $EC_{50}$ value dropped to 7 mM (Figure 2D). Similar behavior was observed with COR-treated traps. These results indicate that

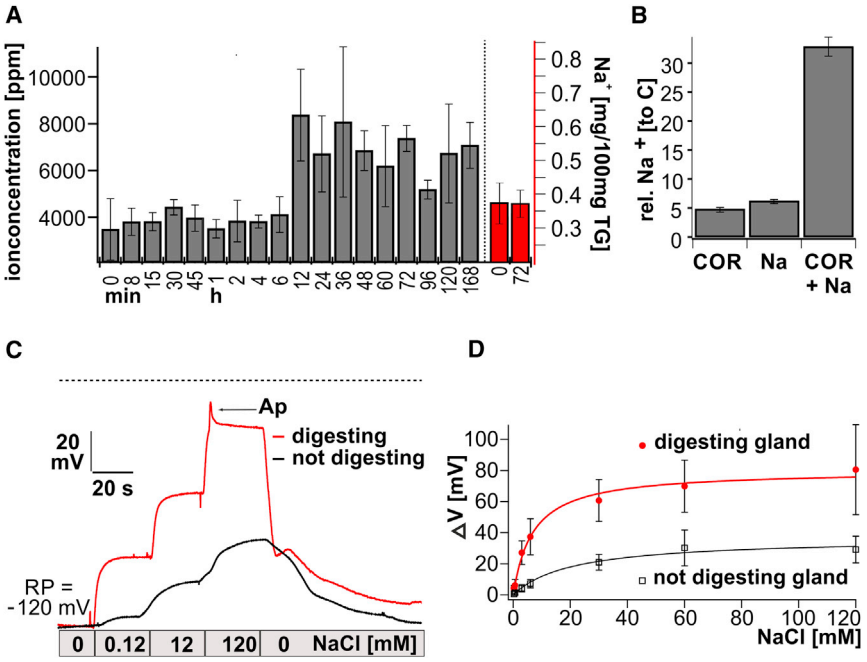


**Figure 2. Sodium Uptake into Stimulated Venus Flytraps Is Elevated**

(A) The time-dependent sodium uptake was analyzed in feeding experiments. After 12 hr of digestion, the $Na^+$ concentrations in fed traps doubled compared to unfed traps (gray bars) (time = 0). The sodium content in *Dionaea* petioles did not increase when traps were fed for 3 days (red bars) ($n \geq 5$, mean ± SD).

(B) Glands treated with coronatine and 1.15 μmol sodium (23 mM in 50 μl) in combination exhibit a higher sodium content compared to the single treatments (relative to carbon) (n = 150, 50 glands per treatment, ±SD).

(C) Impalement measurements on *Dionaea* glands in intact traps revealed more pronounced sodium-dependent membrane depolarizations in digesting (red) traps compared to non-digesting (black) traps.

(D) Quantification of the membrane potential changes ($_{\Delta}V$) in digesting (red) and non-digesting (black) glands in response to varying $Na^+$ concentrations. Data points were acquired by impalement recordings as shown in (C) ($n \geq 5$, mean ± SD). $EC_{50}$ values were calculated by fitting the data points with a Michaelis-Menten equation. Digesting glands were characterized by a half maximal depolarization ($EC_{50}$) at a sodium concentration of 6.86 ± 1.05 mM, while non-digesting cells exhibited an $EC_{50}$ value of 20.70 ± 5.09 mM. See also Table S1.

the plasma membrane of gland cells operates a sodium conductance that is induced upon insect or COR stimulation of the flytrap.

## Flytrap Contact with Prey Induces Gland Cell Expression of a Sodium-Selective Channel

To test whether *Dionaea* in general and glands in particular express sodium channels, we searched a *Dionaea muscipula* expressed sequence tag (EST) collection [46]. Although we did not find any animal-type sodium channel sequences [47, 48], we were able to identify an ortholog of the Trk/Ktr/HKT family (Figure S2). We named this flytrap isoform DmHKT1 (GenBank: KT223138) (after the first plant study naming it HKT1 and the convention agreement in the plant field) [49].

## Electrical Excitement Induces Nutrient Transporter Biosynthesis

Building on the finding that insect capture and digestion is associated with ongoing mechanical stimulation, we analyzed the expression of DmHKT1 as a function of the number of experimentally induced APs. In untreated Venus flytraps (0 APs), negligible expression (147 molecules/10,000 actin) of DmHKT1 was observed (Figure 3A). Application of up to three APs did not increase the expression substantially either. When we simulated the situation with a captured insect (cf. Figure 1A) by eliciting between 5 and 60 APs, trap expression of DmHKT1 increased up to 60-fold (Figure 3A). Thus, mechanical stimulation triggers DmHKT1 expression and $Na^+$ uptake. That COR-MO prevented mechano-electric stimulation of DmHKT1 expression suggests that this process is controlled by the JA-signaling pathway (Figure 3A, red bars). This assumption is further supported by our finding of COR-induced secretion and distinct induced DmHKT1 expression in the trap, and particularly in secreting glands (Figures 3B–3D). The maximal induction of DmHKT1 expression in glands and traps was already observed 4 hr after stimulus onset (Figure 3C). To compare the change in DmHKT1 expression and amplitude of $Na^+$-induced depolarization, we monitored the gland cell membrane properties and trap sodium channel mRNA side by side. We found the same time-dependent increase in both characteristics after COR treatment. The expression of DmHKT1, as well as the sodium-dependent depolarization, increased between 3.5 and 6 hr after COR treatment (Figure 3D). This finding supports the notion that prey-derived $Na^+$ is taken up into the glands of *Dionaea* by DmHKT1. Traps that remained non-stimulated commenced neither secretion nor induction of DmHKT1 expression. In this way, DmHKT1 is particularly expressed in digesting glands, which are known to be responsible for nutrient uptake.

Besides DmHKT1, we have recently shown that the *Dionaea* $NH_4^+$ and $K^+$ transporter expression is also induced by the jasmonate mimic COR [44, 45]. This suggests that the expression of the nutrient-relevant transporter genes is regulated by the mechanically induced JA-signaling pathway. To test this hypothesis, we treated the trap samples with 0 or 60 mechano-electrical stimuli and analyzed DmAMT1 and DmHAK5 transcripts (black bars, Figure S1D). In line with our assumption, the concentration of $NH_4^+$ and $K^+$ transporter mRNA increased upon mechanical stimulation and is inhibited by COR-MO (red bars).

## The Flytrap-Expressed Cation Channel Is $Na^+$ Selective

The results of our differential expression analysis identified the *Dionaea* Trk/Ktr/HKT homolog. Trk/Ktr/HKT-type transporters have been associated with potassium, sodium, and calcium uptake [50]. To test the selectivity of the gland-expressed DmHKT1, we

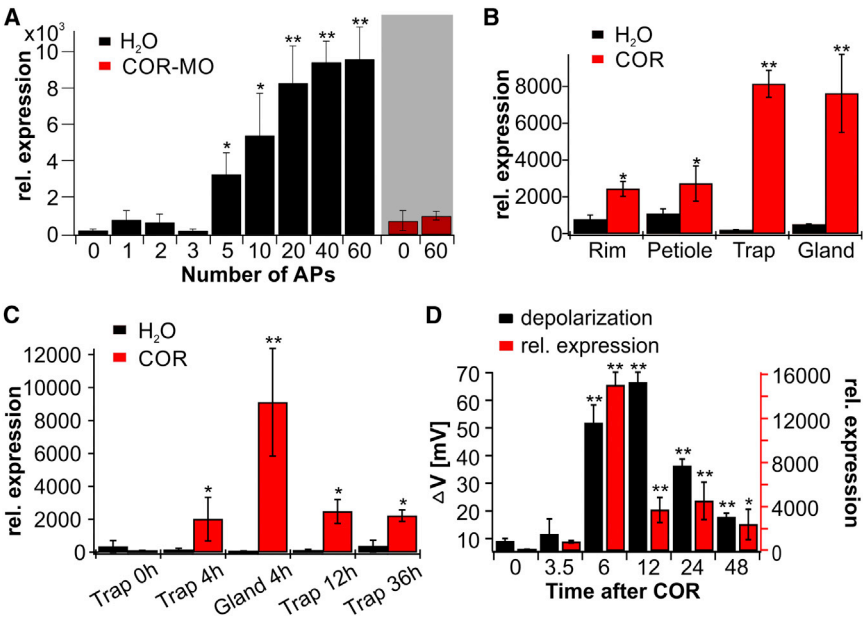


**Figure 3. Expression Pattern of DmHKT1**

(A) The expression level of cation uptake transporter DmHKT1 plotted as a function of the number of mechanical stimulations (as indicated). Traps were pre-treated 4 hr before initiating APs with $H_2O$ (black bars) or the JA pathway inhibitor COR-MO (red). Transcript numbers are given relative to 10,000 molecules of DmACT1. Asterisks indicate a statistically significant difference to zero applied APs (*$p < 0.05$; **$p < 0.01$ by one-way ANOVA) ($n \geq 8$, mean ± SE).

(B) Quantification of DmHKT1 transcript levels in different tissues of the Venus flytrap by qRT-PCR. Asterisks indicate a statistically significant difference to $H_2O$-treated plants (*$p < 0.05$; **$p < 0.01$ by one-way ANOVA) ($n = 3$, mean ± SE).

(C) 4 hr of 100 μM coronatine application stimulated DmHKT1 expression in traps and in isolated glands. Asterisks indicate a statistically significant difference to $H_2O$-treated plants (*$p < 0.05$; **$p < 0.01$ by one-way ANOVA) ($n = 4$, mean ± SE).

(D) Comparison between sodium-dependent membrane depolarizations (black bars) and the relative expression level of DmHKT1 (red bars) in the Venus flytrap in response to COR stimulation. Asterisks indicate a statistically significant difference to zero applied APs (*$p < 0.05$; **$p < 0.01$ by one-way ANOVA) ($n = 4$, mean ± SE). DmHKT1 transcripts were normalized to 10,000 molecules of DmACT1.

See also Figure S2.

injected its cRNA into *Xenopus* oocytes. DmHKT1-expressing oocytes were analyzed using the same protocols as established for *Dionaea* glands (Figures 2C and 2D). Initially, frog oocytes were clamped at −140 mV (the approximate resting potential of *Dionaea* glands) and exposed to 5 mM sodium buffer. In response to the sodium ions, inward currents of up to −4 μA were evoked in "DmHKT1 oocytes," but not in controls (Figure 4A). Under current-clamp conditions, the inward movement of the positively charged sodium ions depolarized the oocyte plasma membrane in 100 mM NaCl by about 100 mV (Figure S3A).

To elucidate the affinity of DmHKT1 for the sodium permeation process, we increased the external $Na^+$ concentration stepwise from 1 to 100 mM in oocytes expressing the *Dionaea* $Na^+$-selective channel and monitored the change in the membrane potential (Figure S3A). By concurrently fitting the resulting $Na^+$ and voltage-dependent current responses with a Michaelis-Menten equation, a $K_m$ value of 10 mM was calculated (Figures 4B and S3B) at a membrane potential of −140 mV (Figure 2C). This affinity obtained with DmHKT1-expressing oocytes is well in line with the sodium affinity characterized in the stimulated flytrap (Figure 2D).

To quantify the kinetics of sodium transport through gland cells in planta (Figure 4C), we used the microelectrode ion flux measuring (MIFE) technique [51, 52]. We increased the extracellular $Na^+$ concentration stepwise from 0 to 50 mM and followed the net flux changes. When applied to non-stimulated and non-secreting traps, no concentration-dependent flux of $Na^+$ was observed. Only when traps were pre-treated by the prey surrogate COR was the elevation of the external $Na^+$ level followed by a concentration-dependent influx of the sodium ion (Figures S3C and 4C).

Since captured insects are naturally rich in sodium and potassium, we sought to simulate the condition in *Dionaea's* green stomach when animals are decomposed into their components by exposing DmHKT1 oocytes to both these alkali cations. In contrast to $Na^+$, the application of $K^+$ within the same concentration range did not evoke DmHKT1-type inward currents (Figure S3D). Notably, no DmHKT1-mediated electrical responses in the presence of sodium could be detected, even with a $K^+$ concentration ten times higher than that used for $Na^+$ (Figure 4D). In response to changes in the extracellular $Na^+$ concentration from 1 to 10 and 10 to 100 mM, the reversal potential of the sodium current shifted by 54.7 mV (±0.94 mV) and 55.3 mV (±0.94 mV), respectively, in the heterologous *Xenopus* oocytes expression system (Figure S3E). This near-Nernstian behavior of the reversal potential provides biophysical evidence for the operation of DmHKT1 as an ion channel, like its bacterial homolog TrkH [53, 54]. This notion was further confirmed by determining the activation energy (Figure S3F). The $Q_{10}$ value is a unit-less quantity that distinguishes Nernstian-type ion channel transport events from carrier-mediated ones on the basis of their activation energy. Changes in the temperature profile only weakly affected DmHKT1-dependent $Na^+$ currents (Figure S3F), and the $Q_{10}$ value of 1.27 ± 0.01, derived from Arrhenius plotting, clearly classifies the gland cell sodium transport activity as channel-like [44, 45].

In line with the $Na^+$ selectivity of DmHKT1, sodium exposure of excitable gland cells changed neither the amplitude nor the shape of the AP, excluding $Na^+$ as a charge carrier of the *Dionaea* AP [53]. In other words, the consumption of sodium-rich food appears not to affect the AP-based information management of the flytrap.

## DISCUSSION

### How Is an Appropriate Cost-Benefit Balance Maintained during Insect Capture?

Carnivorous plants that depend on animal food should compensate or even exceed the cost of their carnivorous life cycle. Such

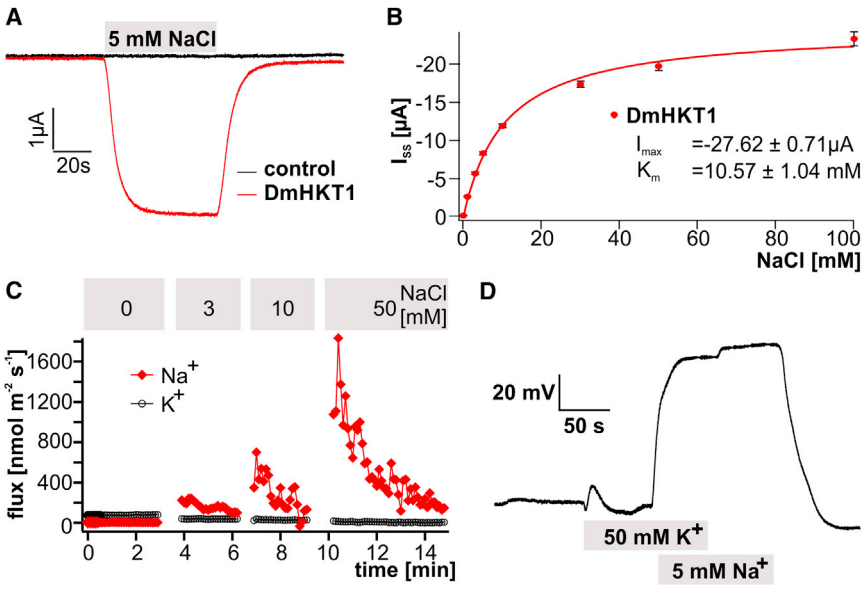


**Figure 4. Electrophysiological Characterization of DmHKT1 Expressed in *Xenopus* Oocytes and Sodium Flux Measurements in *Dionaea* Glands**

(A) Representative sodium-induced inward currents at a membrane potential of −140 mV could be recorded in DmHKT1-expressing oocytes (red line), while water-injected cells (control) did not show sodium-dependent current responses (black line).

(B) Steady-state currents ($I_{SS}$) recorded from DmHKT1-expressing oocytes at −140 mV were plotted as a function of the sodium concentration, and the saturation curve was fitted with a Michaelis-Menten equation. This gave a $K_m$ value of 10 mM ± 1.04 for sodium ions (n = 3, mean ± SD).

(C) MIFE experiments with COR-treated *Dionaea* traps were performed to simultaneously record net $Na^+$ and $K^+$ influxes in response to varying external $Na^+$ concentrations, as indicated in the figure. Increasing external sodium concentrations elevated $Na^+$ influxes up to peak values of ~1,800 nmol $m^{-2}$ $s^{-1}$. In contrast, $K^+$ fluxes were unaffected by changes in the external $Na^+$ concentration, remaining close to 0. A representative MIFE measurement from 12 independent measurements is shown.

(D) Representative membrane potential measurement from a DmHKT1-expressing oocyte revealed $Na^+$-specific membrane potential depolarizations. The perfusion protocol is given within the figure, and the osmolarity was maintained at 240 mOsm/kg with NMDG-Cl.

See also Figure S3.

expenses include trap generation, maintenance, and prey processing, and these must be balanced by the energy gained from the captured animal. To prevent any imbalance (i.e., net energy loss), *Dionaea* controls the processes in its capture organ via trap-specific mechano-electric and touch hormonal signaling. In this system, occasional single trigger-hair stimulation is recognized as subthreshold signal and memorized; it does not provide sufficient information to justify closing the trap. In contrast, two mechano-electric signals received within about 30 s of each other are judged sufficient to close the trap. The fast biomechanics of closure are now well understood, but not the cellular mechanisms that induce the destabilization of the metastable, open trap [55–57]. In this work, we did not focus on the molecular events involved in fast trap closure but the subsequent endocrine processes in the glands. Activating the glands to produce and secrete nitrogen-rich digestive enzymes is inherently costly; thus, this process appears to be closely controlled. In the carnivorous plant Nepenthes, the proteolytic activity required to digest the prey seems to be induced and regulated by jasmonate [58]. When the second AP was received right after the initial one, the flytrap closed. At the same time, the electrical closing stimulus induced differential expression of JA receptor COI1 and co-receptor JAZ1. The induction of JAZ1 and the repression of DmCOI1 may be a part of a negative regulatory feedback loop. It has been shown that gland cells that receive a series of at least three APs increase their cytoplasmic calcium level [5]. A rise in calcium has been found to be associated with wounding-induced JA biosynthesis in non-carnivorous plants such as *Arabidopsis* [13–16, 59]. An accumulation of jasmonates has been described as insect induced in the carnivorous sundew plant [7]. Thus, the mechano-electric stimulation of the green stomach via JA signaling triggers transcription of prey-degrading enzymes. Interestingly, expression of such hydrolases is coupled to that of the transporters required for nutrient uptake; prey movement, which we simulated with "5-plus-X" consecutive APs, triggers the de novo synthesis of the sodium channel DmHKT1 (Figure 3A).

## Mechanical Signaling in the Flytrap

In leaves of non-carnivorous plants such as *Arabidopsis*, a locally applied touch stimulus triggers an increase in both cytoplasmic calcium and JA signaling in the stimulated area as well as systemically in defined, directly connected leaves [18, 19]. However, the point where touch ends and wounding starts is difficult to define, but when the stimulus results in wounding, defense genes in both the "local" leaf receiving the stimulus and in non-treated "systemic" leaves are activated [60]. The long-distance signaling of wounding by herbivores is, for example, associated with a stimulus-induced traveling electrical wave [61]. Although the knowledge regarding touch signaling in the model plant *Arabidopsis* is still rather fragmentary, our present data obtained from *Dionaea* allow us to propose the first working model of touch signaling in the flytrap.

We have demonstrated that the mechanical energy is received at the multicellular trigger hair and converted into an electrical signal, an AP. The APs originating from the trigger hair on one lobe travel through the entire trap to reach two major targets: (1) the motor tissue, which initiates fast trap closure and the formation of the green stomach, and (2) the glands, the endocrine system responsible for the prolonged processing of the nutrient and sodium-rich animal meal. Pre-treating traps with COR-MO suppressed AP-induced stomach formation and the filling of the stomach with the lytic moiety. Such COR-MO traps, even when having received as many as 60 mechano-electric stimuli,

reopen, similar to the reopening of untreated traps after the two APs required for the initial close. When we administered an increasing number of stimuli, we found COI1/JAZ1 expression was altered after only two APs, while to achieve a significant differential expression of the hydrolases and nutrient and sodium transporters, about five APs were required. Based on this behavior, we place the induction of genes operating in the endocrine system downstream of JA biosynthesis and signaling.

### *Dionaea* Trap's $Na^+$ Channel Is Capable of Processing Prey-Derived Sodium Loads

We have been able to show that stimulated flytraps acquire and accumulate prey-derived sodium (Figures 2, 4C, and S3C) via a *Dionaea* sodium channel (DmHKT1), which operates in gland cells (Figure 3). The expression of the channel is induced during the process of prey capture and digestion, providing the gland cells with the necessary capacity to take up the animal $Na^+$ released during decomposition of the insect (Figure 2A). Mechanical stimulation by prey induces HKT1 expression (Figure 3A). During this resorption phase, sodium is taken up by the glands and channeled into traps, while the sodium content in the petioles does not change (Figure 2). Thus, sodium is most likely stored in the large central vacuoles of the parenchyma cells.

## Conclusions

Together, these findings suggest that a moving object is identified as a struggling $Na^+$-rich animal trying to escape the trap. As a result, touch-number-induced expression and production of digestive enzymes is accompanied by an increase in the number of DmHKT1 transporters. Sodium uptake and storage in the trap parenchyma of carnivorous *Dionaea* is reminiscent of the salt management by the succulent-leaf-type halophytes [62, 63]. In halophyte species, $Na^+$ can play a beneficial role in metabolic and osmotic functions and can be used as a "cheap osmoticum." Furthermore, optimal growth and yield is observed in the presence of 100–200 mM NaCl in the soil solution [64, 65], and some of these plants can accumulate substantial (in excess of 1 M on a fresh weight [FW] basis) amounts of $Na^+$ in their shoot tissues. Thus, assuming plants possess an efficient mechanism for vacuolar $Na^+$ sequestration, a high $Na^+$ content in plant tissues is not necessarily associated with toxicity or any detrimental effects. In the case of *Dionaea* plants that live in $K^+$-depleted soils, $Na^+$ could be a substitute cation that enables efficient osmotic adjustment. Thus, *Dionaea* appears to take advantage of $Na^+$ intake for maintaining its cellular osmotic potential and turgor.

## EXPERIMENTAL PROCEDURES

### Surface Potential Measurements

To quantify APs in the Venus flytrap, we used non-invasive surface potential electrodes. One silver electrode was fixed with tape to the outer trap surface with the electrical connection improved by applying a droplet of Kontakt-Gel (Laboklinika). The reference electrode was put into the wet soil. Electrical signals were amplified 100× and recorded with PatchMaster software (HEKA).

### Feeding Experiments

The sodium uptake capacity of traps was determined by feeding traps with insect powder containing defined amounts of the respective cation. Five traps per plant were fed with 20 mg insect powder, dissolved in 100 μl water. The insect powder was derived from adult moths of *Vanessa cardui* (Lep.: Nymphalidae) and had an approximate $Na^+$ content of 5 mM. At the given time points after feeding, traps were harvested, the remaining insect material was removed, and the plant tissue was thoroughly dried. The ground plant powder was then hydrolyzed with $HNO_3$ in a pressure ashing device (Seif). Traps diluted with $H_2O$ were analyzed by ICP-OES (JY 70 Plus, Devision d'Instruments S.A., Jobin Yvon), and petioles of fed traps were analyzed by flame atom absorption spectrometer (F-AAS) (AAnalyst 400, PerkinElmer).

### Laser-Ablation ICP-MS

The laser ablation inductively coupled plasma mass spectrometry (LA-ICP-MS) has been described elsewhere [66]. In brief, *Dionaea* traps on intact plants were treated with 1.15 μmol sodium (in 50 μl; 23 mM), coronatine 100 μM, or sodium and coronatine together for 3 days. Glands were ablated using a solid state NYAG laser (UP193 SS, New Wave Research). $^{13}C$ and $^{23}Na$ signals were detected using the quadrupole ICP-MS (7500 CX, Agilent Technologies), with the $^{13}C$ signal serving as the internal standard.

### Cloning of DmHKT1

Searching the available expressed sequence tag (EST) data from *Dionaea muscipula* [30, 46] revealed a coding sequence related to HKT1-like sodium transporters. PolyA-mRNA was isolated from 10 μg of total RNA using Dynabeads (Invitrogen) according to the manufacturer's instructions. cDNA was generated from *Dionaea muscipula* whole-plant mRNA. The cDNA of DmHKT1 was amplified using gene-specific oligonucleotide primers, which comprised the coding DNA sequence (CDS) of DmHKT1, and Advantage cDNA polymerase mix (Clontech). This revealed a sequence identical to that expected from the EST data. The full-length clone was inserted into pGEM-T Easy using the pGEM-T Easy Vector System I (Promega). For heterologous expression in *Xenopus* oocytes, the generated cDNA of DmHKT1 was cloned into oocyte expression vectors (based on pGEM vectors) using the advanced uracil-excision-based cloning technique described by Nour-Eldin et al. [67]. For functional analysis, cRNA was prepared using the mMessage mMachine T7 Transcription Kit (Ambion). For oocyte electrophysiological experiments, 25 ng of DmHKT1 cRNA was injected and expressed for 2–3 days.

### Synthesis of COR-MO

COR-MO was synthesized according to Monte [38]. All chemicals used were obtained from Sigma-Aldrich. Briefly, 1 mg coronatine was dissolved in ca. 350 μl dried pyridine, and 90 mg solid O-methylhydroxylamine hydrochloride (350 molar excess) was added. The reaction mixture was incubated at 23°C for 18 hr. Non-reacted O-methylhydroxylamine hydrochloride was removed by adding 400 μl water. The product COR-MO was extracted three times from pyridine-water solution using ethyl acetate. The pooled ethyl acetate fraction was washed with water and then dried over sodium sulfate. Thereafter, the solvent was removed by desiccation in vacuo. Conformation of the product was provided by $^1H$ and $^{13}C$ nuclear magnetic resonance (NMR) spectroscopy and compared with published spectral data [38].

### Plant Material and Tissue Sampling

*Dionaea muscipula* plants were purchased from CRESCO Carnivora and grown in plastic pots at 22°C in a 16:8 hr light:dark photoperiod. The material for the expression analyses was harvested as follows: traps, petioles, and trap rims were separated and immediately frozen in liquid nitrogen. Additionally, secretory cells were isolated from the inner trap surface by gently abrading the gland complexes with a razor blade. For induction of secretion and the signal compound treatment, 100 μM COR or the compound solution (Sigma-Aldrich) was directly sprayed onto the respective tissues, and samples were harvested after 24 hr or at the given time points. In inhibitor tests, 100 μM COR-MO was sprayed 4 hr before mechanical stimulation was applied to the Venus flytraps. For mechanical induction of expression, trigger hairs were stimulated 1–60 times (1/min), and samples were collected 4 hr after the first stimulus. Harvested tissue was immediately frozen in liquid nitrogen.

### Expression Analyses

Total RNA was separately isolated from each sample and transcribed into cDNA using M-MLV reverse transcriptase (Promega). Quantification of the actin transcript DmACT1 (GenBank: KC285589) and *Dionaea* transcripts was

performed by real-time PCR as described elsewhere [68]. *Dionaea* transcripts were normalized to 10,000 molecules of DmACT1.

### Non-invasive Ion Flux Measurements

Net fluxes of $Na^+$ and $K^+$ were measured using the non-invasive MIFE technique (University of Tasmania, Australia). The theory of non-invasive MIFE measurements and all specific details of microelectrode fabrication and calibration are available in our prior publications [51, 52, 69]. Briefly, microelectrodes with an external tip diameter of ~2 μm were pulled, silanized and filled with an appropriate ion-selective cocktail. For $K^+$ we used the commercially available cocktail from Sigma: 60031, while for $Na^+$, we used a highly $Na^+$-selective resin that is not responsive to $K^+$ [70]. Electrodes were calibrated with an appropriate set of standards and mounted on a 3D micromanipulator (MMT-5, Narishige). An immobilized lobe was placed into a 90-mm Petri dish containing 40 ml basic salt media (BSM: 0.2 mM KCl, 0.1 mM $CaCl_2$, adjusted to the required pH using Mes/Tris) and placed into a Faraday cage. $Na^+$- and $K^+$-selective microelectrodes were positioned with their tips aligned, 50 μm above the lobe surface using a 3D hydraulic manipulator. During measurement, a computer-controlled stepper motor moved the electrodes in a slow (10 s) square-wave cycle between the two positions, close to (50 μm) and away from (150 μm) the trap surface. The potential difference between two positions was recorded by the MIFE CHART software [51] and converted to an electrochemical potential difference using the calibrated Nernst slopes of the electrodes. Net ion fluxes were calculated using the MIFEFLUX software for cylindrical diffusion geometry [71].

To study the dose dependence of $Na^+$ uptake, intact *Dionaea* leaves were pre-treated with coronatine for 24 hr as described above. A single lobe was cut and immobilized in a measuring chamber using medical adhesive (VH355, Ulrich AG). The lobe was left for adaptation in BSM solution before flux measurements commenced. Net $Na^+$ and $K^+$ fluxes were measured in response to the consecutive increase in NaCl content in the external BSM (NaCl, mM: 0, 3, 10, 50 mM) for 3 min at each NaCl concentration. The pH of the media was maintained at pH 5. Leaves without coronatine treatment were used as controls.

### Intracellular Measurements

Prior to measurement, the lobe of a cut trap was glued to the base of a chamber and left to recover (30 min) in a plant-standard solution containing 0.1 mM KCl, 10 mM $CaCl_2$, and 15 mM MES, adjusted with Tris to pH 6. Osmolarity was maintained at 240 mOsm/kg with D-sorbitol when needed. The NaCl addition to the standard solution was at mM concentrations: 0.3, 0.6, 1.2, 3, 6, 12, 30, 60, 120. During experiments, leaves were continuously perfused with the plant-standard solution (1 ml/min). For stimulation, a 1-min exposure to the respective NaCl concentration was sufficient.

### Oocyte Recordings

For double-electrode voltage-clamp studies (DEVC), oocytes were perfused with Tris/Mes-based buffers. The standard bath solution contained 10 mM Tris/Mes (pH 5.6), 1 mM $CaCl_2$, 1 mM $MgCl_2$, and 1 mM $LaCl_3$. The osmolality of each solution was adjusted to 220 mosmol/kg using D-sorbitol. To balance the ionic strength for measurements under varying cation ($Na^+$ and $K^+$) concentrations, we compensated with lithium to 100 mM. Solutions for selectivity measurements were composed of the standard bath solution supplemented with 100 mM $Na^+$, $NMDG^+$ (N-methyl-d-glucamine), $Li^+$, $K^+$, $Rb^+$, or $Cs^+$ chloride salts. For current-voltage relations (IV-curves), single-voltage pulses were applied in 10 mV increments from −200 to +60 mV after starting from a holding potential ($V_H$) of 0 mV. Steady-state currents ($I_{SS}$) were extracted at the end of the test pulses lasting 50 ms. Temperature experiments were performed under standard solution conditions as described by Scherzer et al. [45]. The $Q_{10}$ value is proportional to the free energy of activation ($_{\Delta}G$), and it is the factor by which the transport rate increases when the temperature is changed by ten degrees. The only known transport processes for small hydrophilic ions with $Q_{10}$ values below 2.0 are catalyzed by channel proteins. Data were analyzed using Igor Pro and Origin Pro 9.0G.

## SUPPLEMENTAL INFORMATION

Supplemental Information includes three figures and one table and can be found with this article online at http://dx.doi.org/10.1016/j.cub.2015.11.057.

## AUTHOR CONTRIBUTIONS

J.B. and S. Scherzer contributed equally to this work. E.N. and R.H. conceived the work. S. Scherzer and J.B. conducted initial feasibility studies. J.B., S. Scherzer, E.K., I.K., L.S., K.v.M., C.L., S. Shabala, K.A.S.A.-R., R.H., T.D.M., E.N., and H.R. designed the experiments and analyzed the data. S. Scherzer, J.B., E.K., L.S., K.v.M., and C.L. performed the experiments. S. Scherzer, J.B., E.N., K.A.S.A.-R., S. Shabala, and R.H. wrote the manuscript. I.M. and R.S. provided samples of COR-MO and revised the manuscript.

## ACKNOWLEDGMENTS

We thank B. Neumann, S. Kopp, and M. v. Rüden for excellent assistance; A. Specht (Institute of Plant Nutrition, Leibniz University Hannover) for assistance during the laser ablation ICP-MS-experiments; and Prof. W. Boland (Max Planck Institute for Chemical Ecology) for providing us with the JA derivatives. The authors thank M. Gruene (Institute for Organic Chemistry, University of Wuerzburg) for acquisition of NMR data. This work was supported by the European Research Council under the European Union's Seventh Framework Programme (FP/20010-2015)/ERC Grant Agreement no. 250194-Carnivorom. Work in R.S. lab is supported by grant BIO2013-44407-R from MINECO. This work was also supported by the International Research Group Program (IRG14-08), Deanship of Scientific Research, King Saud University (to R.H., E.N., and K.A.S.A.-R.) and by grants of the Australian Research Council (project DP150101663) and the Grain Research and Development Corporation (to S. Shabala).

Received: June 12, 2015
Revised: October 23, 2015
Accepted: November 26, 2015
Published: January 21, 2016

## REFERENCES

1. Tretner, C., Huth, U., and Hause, B. (2008). Mechanostimulation of *Medicago truncatula* leads to enhanced levels of jasmonic acid. J. Exp. Bot. *59*, 2847–2856.
2. Weiler, E.W., Albrecht, T., Groth, B., Xia, Z.-Q., Luxem, M., Liß, H., Andert, L., and Spengler, P. (1993). Evidence for the involvement of jasmonates and their octadecanoid precursors in the tendril coiling response of *Bryonia dioica*. Phytochemistry *32*, 591–600.
3. Chehab, E.W., Yao, C., Henderson, Z., Kim, S., and Braam, J. (2012). *Arabidopsis* touch-induced morphogenesis is jasmonate mediated and protects against pests. Curr. Biol. *22*, 701–706.
4. Stelmach, B.A., Müller, A., Hennig, P., Laudert, D., Andert, L., and Weiler, E.W. (1998). Quantitation of the octadecanoid 12-oxo-phytodienoic acid, a signalling compound in plant mechanotransduction. Phytochemistry *47*, 539–546.
5. Escalante-Pérez, M., Krol, E., Stange, A., Geiger, D., Al-Rasheid, K.A.S., Hause, B., Neher, E., and Hedrich, R. (2011). A special pair of phytohormones controls excitability, slow closure, and external stomach formation in the Venus flytrap. Proc. Natl. Acad. Sci. USA *108*, 15492–15497.
6. Libiaková, M., Floková, K., Novák, O., Slováková, L., and Pavlovič, A. (2014). Abundance of cysteine endopeptidase dionain in digestive fluid of Venus flytrap (*Dionaea muscipula Ellis*) is regulated by different stimuli from prey through jasmonates. PLoS ONE *9*, e104424.
7. Nakamura, Y., Reichelt, M., Mayer, V.E., and Mithöfer, A. (2013). Jasmonates trigger prey-induced formation of 'outer stomach' in carnivorous sundew plants. Proc. Biol. Sci. *280*, 20130228.
8. Darwin, C. (1875). Insectivorous Plants (D. Appleton & Co.).
9. Kreuzwieser, J., Scheerer, U., Kruse, J., Burzlaff, T., Honsel, A., Alfarraj, S., Georgiev, P., Schnitzler, J.P., Ghirardo, A., Kreuzer, I., et al. (2014). The Venus flytrap attracts insects by the release of volatile organic compounds. J. Exp. Bot. *65*, 755–766.

10. Mariod, A.A., Abdel-Wahab, S.I., and Ain, N.M. (2011). Proximate amino acid, fatty acid and mineral composition of two Sudanese edible pentatomid insects. Int. J. Trop. Insect Sci. *31*, 145–153.
11. Finke, M.D. (2013). Complete nutrient content of four species of feeder insects. Zoo Biol. *32*, 27–36.
12. Yamaguchi, T., Hamamoto, S., and Uozumi, N. (2013). Sodium transport system in plant cells. Front. Plant Sci. *4*, 410.
13. Vadassery, J., Reichelt, M., Jimenez-Aleman, G.H., Boland, W., and Mithöfer, A. (2014). Neomycin inhibition of (+)-7-iso-jasmonoyl-L-isoleucine accumulation and signaling. J. Chem. Ecol. *40*, 676–686.
14. Maffei, M., Bossi, S., Spiteller, D., Mithöfer, A., and Boland, W. (2004). Effects of feeding *Spodoptera littoralis* on lima bean leaves. I. Membrane potentials, intracellular calcium variations, oral secretions, and regurgitate components. Plant Physiol. *134*, 1752–1762.
15. Dombrowski, J.E., and Bergey, D.R. (2007). Calcium ions enhance systemin activity and play an integral role in the wound response. Plant Sci. *172*, 335–344.
16. Fisahn, J., Herde, O., Willmitzer, L., and Peña-Cortés, H. (2004). Analysis of the transient increase in cytosolic $Ca^{2+}$ during the action potential of higher plants with high temporal resolution: requirement of $Ca^{2+}$ transients for induction of jasmonic acid biosynthesis and PINII gene expression. Plant Cell Physiol. *45*, 456–459.
17. Pavlovič, A., and Saganová, M. (2015). A novel insight into the cost-benefit model for the evolution of botanical carnivory. Ann. Bot. (Lond.) *115*, 1075–1092.
18. Reymond, P., Weber, H., Damond, M., and Farmer, E.E. (2000). Differential gene expression in response to mechanical wounding and insect feeding in *Arabidopsis*. Plant Cell *12*, 707–720.
19. Chehab, E.W., Eich, E., and Braam, J. (2009). Thigmomorphogenesis: a complex plant response to mechano-stimulation. J. Exp. Bot. *60*, 43–56.
20. Pauwels, L., and Goossens, A. (2011). The JAZ proteins: a crucial interface in the jasmonate signaling cascade. Plant Cell *23*, 3089–3100.
21. Gfeller, A., Liechti, R., and Farmer, E.E. (2010). *Arabidopsis* jasmonate signaling pathway. Sci. Signal. *3*, cm4.
22. Gimenez-Ibanez, S., Boter, M., and Solano, R. (2015). Novel players fine-tune plant trade-offs. Essays Biochem. *58*, 83–100.
23. Scholz, S.S., Vadassery, J., Heyer, M., Reichelt, M., Bender, K.W., Snedden, W.A., Boland, W., and Mithöfer, A. (2014). Mutation of the *Arabidopsis* calmodulin-like protein CML37 deregulates the jasmonate pathway and enhances susceptibility to herbivory. Mol. Plant *7*, 1712–1726.
24. Chung, H.S., Koo, A.J.K., Gao, X., Jayanty, S., Thines, B., Jones, A.D., and Howe, G.A. (2008). Regulation and function of *Arabidopsis* JASMONATE ZIM-domain genes in response to wounding and herbivory. Plant Physiol. *146*, 952–964.
25. Acosta, I.F., Gasperini, D., Chételat, A., Stolz, S., Santuari, L., and Farmer, E.E. (2013). Role of NINJA in root jasmonate signaling. Proc. Natl. Acad. Sci. USA *110*, 15473–15478.
26. Pauwels, L., Morreel, K., De Witte, E., Lammertyn, F., Van Montagu, M., Boerjan, W., Inzé, D., and Goossens, A. (2008). Mapping methyl jasmonate-mediated transcriptional reprogramming of metabolism and cell cycle progression in cultured *Arabidopsis* cells. Proc. Natl. Acad. Sci. USA *105*, 1380–1385.
27. Benedetti, C.E., Costa, C.L., Turcinelli, S.R., and Arruda, P. (1998). Differential expression of a novel gene in response to coronatine, methyl jasmonate, and wounding in the Coi1 mutant of *Arabidopsis*. Plant Physiol. *116*, 1037–1042.
28. Edreva, A. (2005). Pathogenesis-related proteins: research progress in the last 15 years. Gen. Appl. Plant Physiol. *31*, 105–124.
29. Reymond, P., and Farmer, E.E. (1998). Jasmonate and salicylate as global signals for defense gene expression. Curr. Opin. Plant Biol. *1*, 404–411.
30. Schulze, W.X., Sanggaard, K.W., Kreuzer, I., Knudsen, A.D., Bemm, F., Thøgersen, I.B., Bräutigam, A., Thomsen, L.R., Schliesky, S., Dyrlund, T.F., et al. (2012). The protein composition of the digestive fluid from the venus flytrap sheds light on prey digestion mechanisms. Mol. Cell. Proteomics *11*, 1306–1319.
31. Paszota, P., Escalante-Perez, M., Thomsen, L.R., Risør, M.W., Dembski, A., Sanglas, L., Nielsen, T.A., Karring, H., Thøgersen, I.B., Hedrich, R., et al. (2014). Secreted major Venus flytrap chitinase enables digestion of Arthropod prey. Biochim. Biophys. Acta *1844*, 374–383.
32. Miersch, O., Neumerkel, J., Dippe, M., Stenzel, I., and Wasternack, C. (2008). Hydroxylated jasmonates are commonly occurring metabolites of jasmonic acid and contribute to a partial switch-off in jasmonate signaling. New Phytol. *177*, 114–127.
33. Kitaoka, N., Matsubara, T., Sato, M., Takahashi, K., Wakuta, S., Kawaide, H., Matsui, H., Nabeta, K., and Matsuura, H. (2011). *Arabidopsis* CYP94B3 encodes jasmonyl-L-isoleucine 12-hydroxylase, a key enzyme in the oxidative catabolism of jasmonate. Plant Cell Physiol. *52*, 1757–1765.
34. Koo, A.J., Cooke, T.F., and Howe, G.A. (2011). Cytochrome P450 CYP94B3 mediates catabolism and inactivation of the plant hormone jasmonoyl-L-isoleucine. Proc. Natl. Acad. Sci. USA *108*, 9298–9303.
35. Radhika, V., Kost, C., Boland, W., and Heil, M. (2010). The role of jasmonates in floral nectar secretion. PLoS ONE *5*, e9265.
36. Heil, M., Koch, T., Hilpert, A., Fiala, B., Boland, W., and Linsenmair, K. (2001). Extrafloral nectar production of the ant-associated plant, Macaranga tanarius, is an induced, indirect, defensive response elicited by jasmonic acid. Proc. Natl. Acad. Sci. USA *98*, 1083–1088.
37. Wasternack, C., and Hause, B. (2013). Jasmonates: biosynthesis, perception, signal transduction and action in plant stress response, growth and development. An update to the 2007 review in Annals of Botany. Ann. Bot. (Lond.) *111*, 1021–1058.
38. Monte, I., Hamberg, M., Chini, A., Gimenez-Ibanez, S., García-Casado, G., Porzel, A., Pazos, F., Boter, M., and Solano, R. (2014). Rational design of a ligand-based antagonist of jasmonate perception. Nat. Chem. Biol. *10*, 671–676.
39. Wright, E.M., Hirayama, B.A., and Loo, D.F. (2007). Active sugar transport in health and disease. J. Intern. Med. *261*, 32–43.
40. Harada, N., and Inagaki, N. (2012). Role of sodium-glucose transporters in glucose uptake of the intestine and kidney. J. Diabetes Investig. *3*, 352–353.
41. Kruse, J., Gao, P., Honsel, A., Kreuzwieser, J., Burzlaff, T., Alfarraj, S., Hedrich, R., and Rennenberg, H. (2014). Strategy of nitrogen acquisition and utilization by carnivorous *Dionaea muscipula*. Oecologia *174*, 839–851.
42. Lloyd, F.E. (1942). The Carnivorous Plants (Chronica Botanica Company).
43. Finke, M.D. (2002). Complete nutrient composition of commercially raised invertebrates used as food for insectivores. Zoo Biol. *21*, 269–285.
44. Scherzer, S., Böhm, J., Krol, E., Shabala, L., Kreuzer, I., Larisch, C., Bemm, F., Al-Rasheid, K.A., Shabala, S., Rennenberg, H., et al. (2015). Calcium sensor kinase activates potassium uptake systems in gland cells of Venus flytraps. Proc. Natl. Acad. Sci. USA *112*, 7309–7314.
45. Scherzer, S., Krol, E., Kreuzer, I., Kruse, J., Karl, F., von Rüden, M., Escalante-Perez, M., Müller, T., Rennenberg, H., Al-Rasheid, K.A., et al. (2013). The Dionaea muscipula ammonium channel DmAMT1 provides $NH_4^+$ uptake associated with Venus flytrap's prey digestion. Curr. Biol. *23*, 1649–1657.
46. Jensen, M.K., Vogt, J.K., Bressendorff, S., Seguin-Orlando, A., Petersen, M., Sicheritz-Pontén, T., and Mundy, J. (2015). Transcriptome and genome size analysis of the Venus flytrap. PLoS ONE *10*, e0123887.
47. Yang, Z., Gu, E., Lu, X., and Wang, J.H. (2014). Essential role of axonal VGSC inactivation in time-dependent deceleration and unreliability of spike propagation at cerebellar Purkinje cells. Mol. Brain *7*, 1.
48. Rossier, B.C. (2014). Epithelial sodium channel (ENaC) and the control of blood pressure. Curr. Opin. Pharmacol. *15*, 33–46.
49. Platten, J.D., Cotsaftis, O., Berthomieu, P., Bohnert, H., Davenport, R.J., Fairbairn, D.J., Horie, T., Leigh, R.A., Lin, H.X., Luan, S., et al. (2006). Nomenclature for HKT transporters, key determinants of plant salinity tolerance. Trends Plant Sci. *11*, 372–374.

50. Almeida, P., Katschnig, D., and de Boer, A.H. (2013). HKT transporters–state of the art. Int. J. Mol. Sci. *14*, 20359–20385.

51. Shabala, S.N., Newman, I.A., and Morris, J. (1997). Oscillations in $H^+$ and $Ca^{2+}$ ion fluxes around the elongation region of corn roots and effects of external pH. Plant Physiol. *113*, 111–118.

52. Shabala, S., Demidchik, V., Shabala, L., Cuin, T.A., Smith, S.J., Miller, A.J., Davies, J.M., and Newman, I.A. (2006). Extracellular $Ca^{2+}$ ameliorates NaCl-induced $K^+$ loss from *Arabidopsis* root and leaf cells by controlling plasma membrane $K^+$ -permeable channels. Plant Physiol. *141*, 1653–1665.

53. Böhm, J., Scherzer, S., Shabala, S., Krol, E., Neher, E., Mueller, T.D., and Hedrich, R. (2015). Venus flytrap HKT1-type channel provides for prey sodium uptake into carnivorous plant without conflicting with electrical excitability. Mol. Plant. http://dx.doi.org/10.1016/j.molp.2015.09.017, S1674-2052(15)00394-9.

54. Cao, Y., Pan, Y., Huang, H., Jin, X., Levin, E.J., Kloss, B., and Zhou, M. (2013). Gating of the TrkH ion channel by its associated RCK protein TrkA. Nature *496*, 317–322.

55. Poppinga, S., and Joyeux, M. (2011). Different mechanics of snap-trapping in the two closely related carnivorous plants *Dionaea muscipula* and *Aldrovanda vesiculosa*. Phys. Rev. E Stat. Nonlin. Soft Matter Phys. *84*, 041928.

56. Li, Y., Lenaghan, S.C., and Zhang, M. (2012). Nonlinear dynamics of the movement of the venus flytrap. Bull. Math. Biol. *74*, 2446–2473.

57. Volkov, A.G., Harris, S.L., 2nd, Vilfranc, C.L., Murphy, V.A., Wooten, J.D., Paulicin, H., Volkova, M.I., and Markin, V.S. (2013). Venus flytrap biomechanics: forces in the *Dionaea muscipula* trap. J. Plant Physiol. *170*, 25–32.

58. Buch, F., Rott, M., Rottloff, S., Paetz, C., Hilke, I., Raessler, M., and Mithöfer, A. (2013). Secreted pitfall-trap fluid of carnivorous *Nepenthes* plants is unsuitable for microbial growth. Ann. Bot. (Lond.) *111*, 375–383.

59. León, J., Rojo, E., Titarenko, E., and Sánchez-Serrano, J.J. (1998). Jasmonic acid-dependent and -independent wound signal transduction pathways are differentially regulated by $Ca^{2+}$/calmodulin in *Arabidopsis thaliana*. Mol. Gen. Genet. *258*, 412–419.

60. Mousavi, S.A., Chauvin, A., Pascaud, F., Kellenberger, S., and Farmer, E.E. (2013). GLUTAMATE RECEPTOR-LIKE genes mediate leaf-to-leaf wound signalling. Nature *500*, 422–426.

61. Zimmermann, M.R., Maischak, H., Mithöfer, A., Boland, W., and Felle, H.H. (2009). System potentials, a novel electrical long-distance apoplastic signal in plants, induced by wounding. Plant Physiol. *149*, 1593–1600.

62. Shabala, S., Bose, J., and Hedrich, R. (2014). Salt bladders: do they matter? Trends Plant Sci. *19*, 687–691.

63. Shabala, S. (2011). Physiological and cellular aspects of phytotoxicity tolerance in plants: the role of membrane transporters and implications for crop breeding for waterlogging tolerance. New Phytol. *190*, 289–298.

64. Flowers, T.J., and Colmer, T.D. (2008). Salinity tolerance in halophytes. New Phytol. *179*, 945–963.

65. Shabala, L., Mackay, A., Tian, Y., Jacobsen, S.E., Zhou, D., and Shabala, S. (2012). Oxidative stress protection and stomatal patterning as components of salinity tolerance mechanism in quinoa (*Chenopodium quinoa*). Physiol. Plant. *146*, 26–38.

66. Klug, B., Specht, A., and Horst, W.J. (2011). Aluminium localization in root tips of the aluminium-accumulating plant species buckwheat (*Fagopyrum esculentum Moench*). J. Exp. Bot. *62*, 5453–5462.

67. Nour-Eldin, H.H., Hansen, B.G., Nørholm, M.H.H., Jensen, J.K., and Halkier, B.A. (2006). Advancing uracil-excision based cloning towards an ideal technique for cloning PCR fragments. Nucleic Acids Res. *34*, e122.

68. Escalante-Pérez, M., Jaborsky, M., Lautner, S., Fromm, J., Müller, T., Dittrich, M., Kunert, M., Boland, W., Hedrich, R., and Ache, P. (2012). Poplar extrafloral nectaries: two types, two strategies of indirect defenses against herbivores. Plant Physiol. *159*, 1176–1191.

69. Shabala, S., and Shabala, L. (2002). Kinetics of net H+, Ca2+, K+, Na+, NH+4, and Cl- fluxes associated with post-chilling recovery of plasma membrane transporters in Zea mays leaf and root tissues. Physiol. Plant. *114*, 47–56.

70. Jayakannan, M., Babourina, O., and Rengel, Z. (2011). Improved measurements of $Na^+$ fluxes in plants using calixarene-based microelectrodes. J. Plant Physiol. *168*, 1045–1051.

71. Newman, I.A. (2001). Ion transport in roots: measurement of fluxes using ion-selective microelectrodes to characterize transporter function. Plant Cell Environ. *24*, 1–14.

**Current Biology, Volume *26***

## Supplemental Information

# The Venus Flytrap *Dionaea muscipula* Counts Prey-Induced Action Potentials to Induce Sodium Uptake

**Jennifer Böhm, Sönke Scherzer, Elzbieta Krol, Ines Kreuzer, Katharina von Meyer, Christian Lorey, Thomas D. Mueller, Lana Shabala, Isabel Monte, Roberto Solano, Khaled A.S. Al-Rasheid, Heinz Rennenberg, Sergey Shabala, Erwin Neher, and Rainer Hedrich**

Figure S1

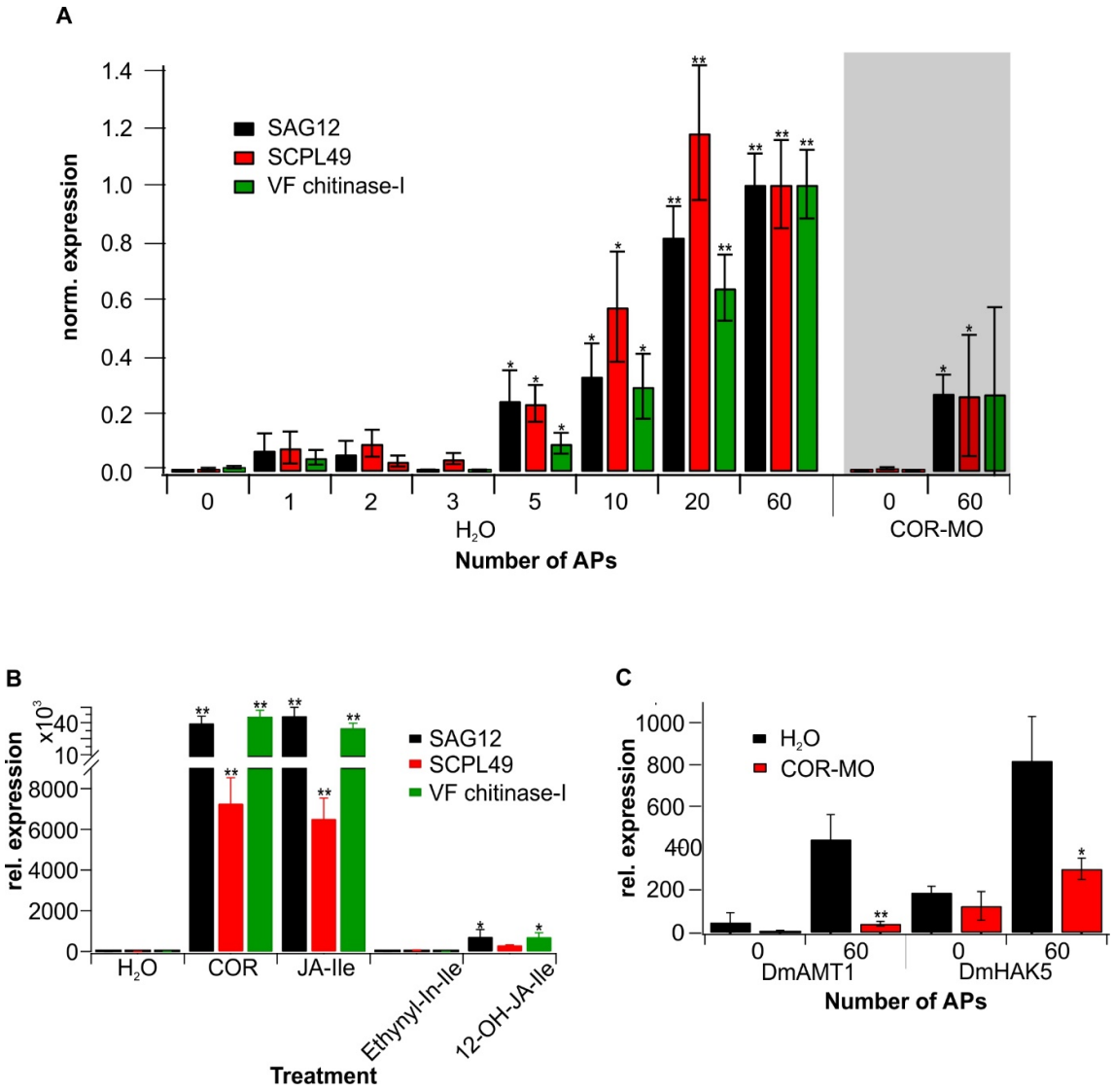


**Fig. S1. Related to Figure 1**

Transcript numbers were normalised to 10,000 molecules of DmACT1. (A): Transcript levels of the *Dionaea* hydrolases SAG12, SCPL49 and VF chitinase-I in response to different number of APs were quantified by qRT-PCR. Traps were pre-treated 4 h before initiating APs with $H_2O$ (shaded in white) or the JA pathway inhibitor COR-MO (shaded in grey). Asterisks indicate a statistically significant difference to zero applied APs (* = $P < 0.05$; ** = $P < 0.01$ by one-way ANOVA) ($n \geq 3$, mean ± SE). (B): Expression level of hydrolases following chemical induction by COR, JA-Ile, Ethynyl-In-Ile and 12-OH-JA-Ile. Control plants were sprayed with water. Asterisks indicate a statistically significant difference to control plants (* = $P < 0.05$; ** = $P < 0.01$ by one-way ANOVA) ($n \geq 3$, mean ± SE). (C): Expression level of DmAMT1 and DmHAK5

after application of 0 and 60 APs. Mechanically-induced gene regulation was inhibited by application of 100 µM COR-MO (red). Control plants (black) were sprayed with water. Asterisks indicate a statistically significant difference to control plants (* = $P < 0.05$; ** = $P < 0.01$ by one-way ANOVA) ($n \geq 4$, mean ± SE).

Figure S2

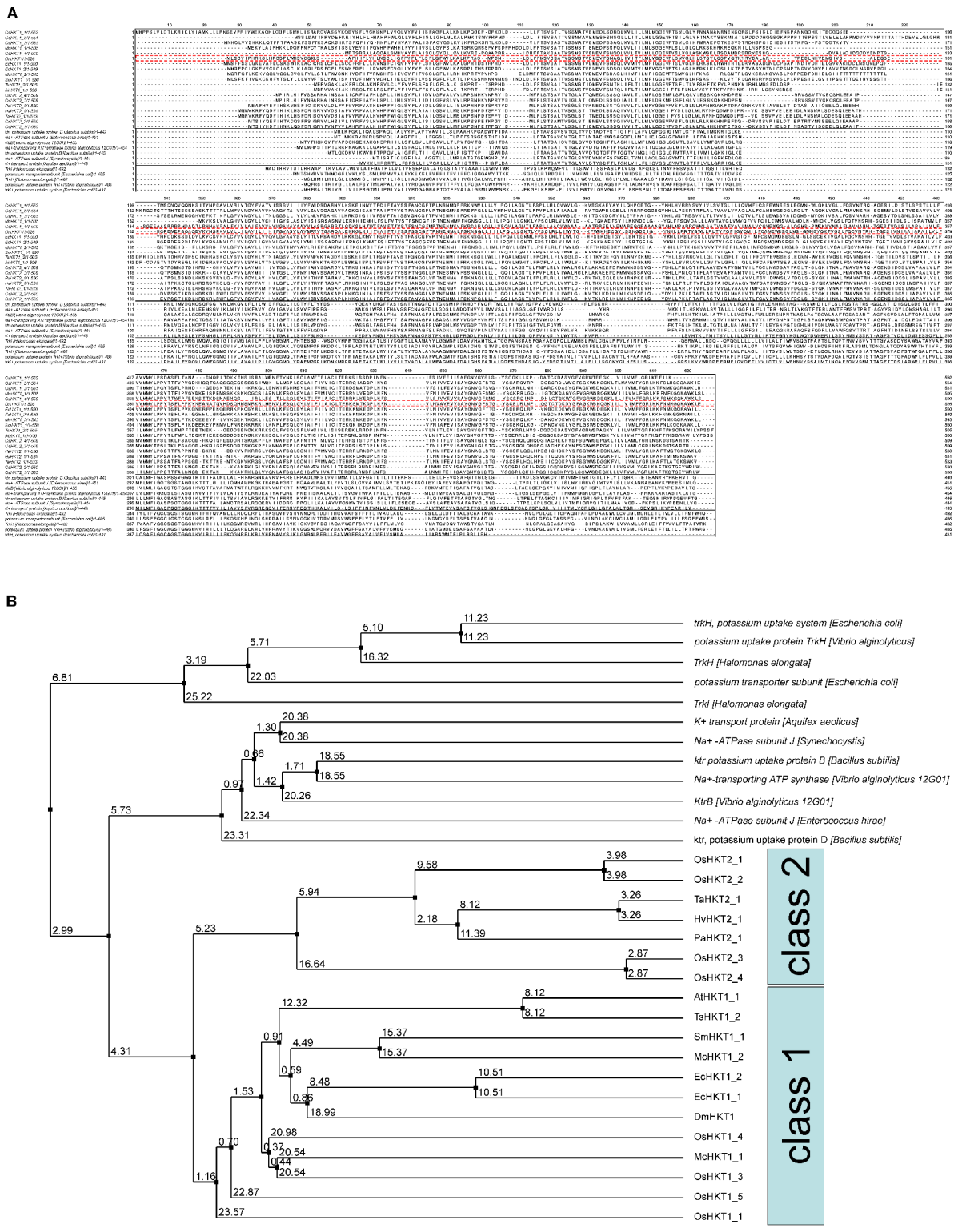


**Fig. S2. Related to Figure 3**

(A): Sequences of Trk/Ktr/HKT orthologues from various plant, bacterial and fungal species were aligned by ClustralW2. HKT1 from *Dionaea muscipula* is boxed in red (jalview 2.7). (B): Phylogenetic relation between Trk/Ktr/HKT transporters. The phylogenetic tree is based on an

alignment with selected protein sequences of plant, bacterial and fungal Trk/Ktr/HKT transporters (as indicated). The tree was constructed with Geneious using Neighbor-Joining [S1].

Figure S3

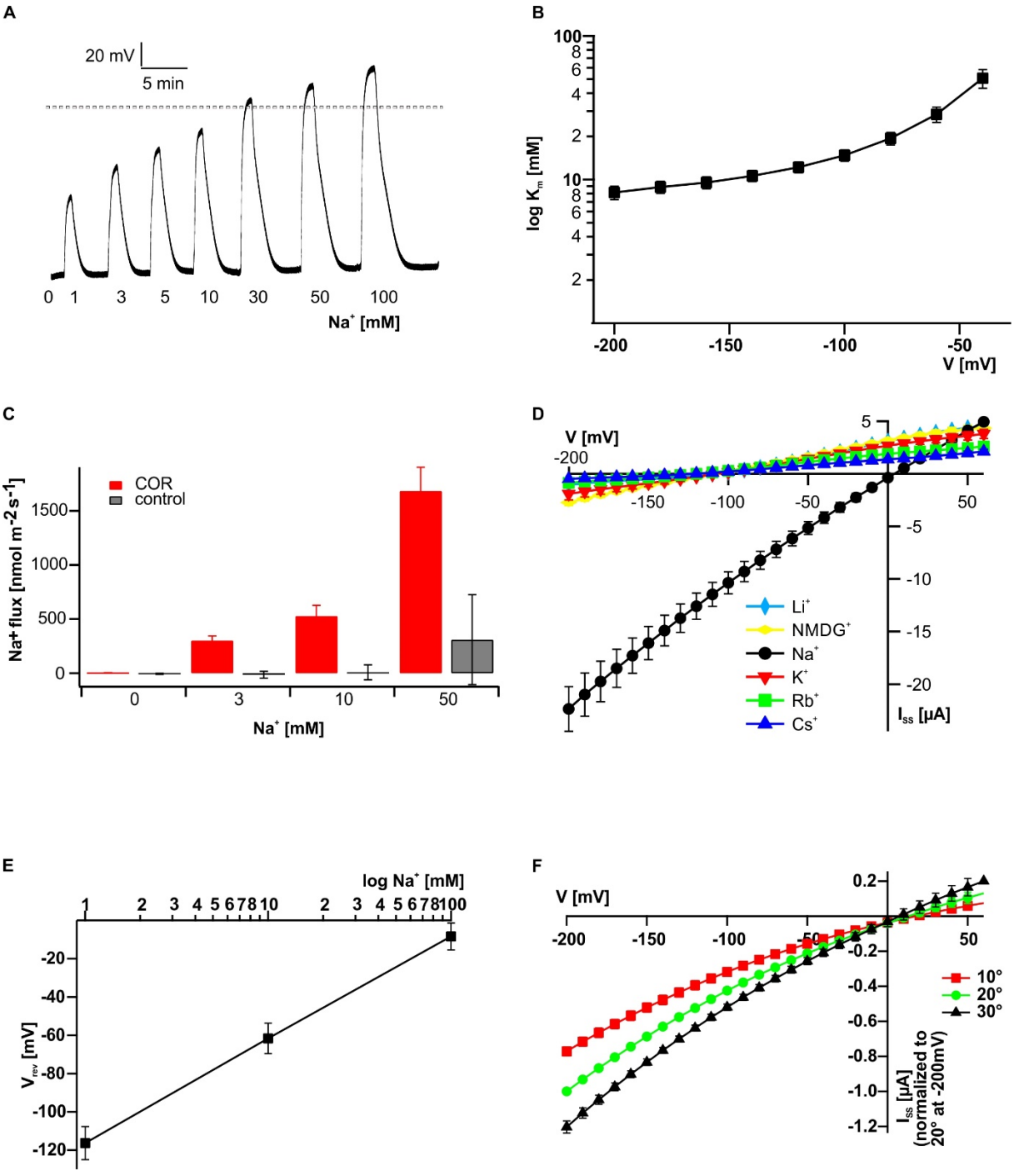


**Fig. S3. Related to Figure 4**

(A): Membrane potential measurements recorded in a representative DmHKT1-expressing oocyte in response to stepwise increases in sodium concentrations as indicated. Between applications of the different sodium concentrations, the oocyte was perfused with 100 mM LiCl. The dotted line indicates 0 mV. (B): $K_m$ values derived from saturation curves recorded at different membrane potentials were fitted with a Michaelis-Menten equation. $K_m$ values were

plotted as a function of the applied voltage, which indicated a pronounced voltage-dependent affinity of DmHKT1 towards sodium ions (n = 3, mean ± SD). (C): Net $Na^+$ fluxes derived from COR stimulated and unstimulated Venus flytraps using the MIFE-technique. COR-stimulated traps mediated $Na^+$ influx at all the tested external sodium concentrations. With 50 mM external NaCl, the sodium influx increased to 1683 ± 218 nmol $m^{-2}$ $s^{-1}$. In contrast, non-stimulated traps showed a $Na^+$ uptake of only 310 ±415 nmol $m^{-2}$ $s^{-1}$ with 50 mM external NaCl (n ≥ 7, mean ± SD). (D): Current-voltage relation in the presence of various monovalent cations (100 mM each) illustrates the sodium-specific conductance of DmHKT1 (n = 3, mean ± SE). (E): The reversal potential ($V_{rev}$) recorded with DmHKT1-expressing oocytes were plotted against the applied sodium concentrations (logarithmic scale) (n = 3, mean ± SD). The reversal potential shifted in a sodium dependent manner with a slope of 54.7 ± 0.94 mV (1 – 10 mM $Na^+$) and 55.3 ± 0.94 (10 – 100 mM $Na^+$), respectively (n = 5, mean ± SD). (F): DmHKT1-mediated sodium currents were recorded at voltages ranging from +60 mV to -200 mV at bath temperatures of 10, 20 and 30 °C in 100 mM NaCl solutions. Data points were normalised to -200 mV at 20 °C and 100 mM $Na^+$. $Q_{10}$ values were calculated at membrane potentials from -50 mV to -200 mV, and as the mean factor between currents recorded at the given temperatures. The mean of the resulting $Q_{10}$ values calculated between 10 °C - 20 °C, 20 °C - 30 °C and √ 10 °C -30 °C was 1.27 ± 0.01 (n = 5, mean ± SD).

Table S1

Ions in moth powder:

| **µmol/g DW** | **Mean±SD** |
|---|---|
| $Ca_2^+$ | 6.11±0.96 |
| $K^+$ | 305.07±66.55 |
| $Mg^+$ | 23.63±5.02 |
| $Na^+$ | 42.64±8.58 |
| $PO_4^{3-}$ | 110.09±32.28 |
| $SO_4^{2-}$ | 6.35±2.1 |
| $NO_3^-$ | 156.07±41.2 |

**Table S1. Related to Figure 2**

The ion content of the standardized animal powder used for feeding experiments shown in Fig 2A. DW: dry weight (n = 5 replicates, mean ± SD).

**Supplemental References**

S1. Ko JH, Yang SH, Han KH (2006) Upregulation of an *Arabidopsis* RING-H2 gene, *XERICO*, confers drought tolerance through increased abscisic acid biosynthesis. Plant J 47: 343-355.